CHANGE DETECTION USING RELATIVE ATMOSPHERIC CORRECTION OF SATELLITE IMAGES AT DIFFERENT TIMES

Takashi Kusaka, Takao Kakehi and Masanori Ootuka
Kanazawa Institute of Technology
Nonoichi-machi Ishikawa 921, JAPAN
E-mail: kusaka@manage.kanazawa-it.ac.jp
Commission VII, Working Group 2

KEY WORDS: CHANGE_DETECTION, LAND_USE, ATMOSPHERIC_CORRECTION, LANDSAT

ABSTRACT:

This study describes a method for detecting land cover change that uses the relative atmospheric correction of multi-temporal satellite images. The radiance change arising from the difference in atmospheric conditions and sun angles between satellite images taken at different times, can be estimated in a relative way, by taking one image as reference.First, it is derived from the radiative transfer model that the relation between radiance values of remotely sensed data acquired at two different dates has a linear form. Next, it is shown that the surface reflectance ratio, A(t2)/A(t1), at two different times, t1 and t2, is evaluated by pixel values, X(t2) and X(t1), the coefficients of the estimated linear equation and the additive path radiance in the image taken as reference. The distance d of A(t2)/A(t1) from the value of 1 was introduced to detect the area of change. The threshold values of d were automatically determined by using the 2-dimensional frequency distribution of distance values in two different spectral bands. Finally, the present method was applied to Landsat TM images taken at Oct. 1987 and Nov. 1991. As a result, it is shown that the areas of land cover change are successfully detected by using the threshold of the distance selected in this study.

1. INTRODUCTION

Land cover change detection is one of the major applications of remotely sensed data and is useful in the analysis of environmental change such as land use change, assessment of deforestation and damage assessment. Several methods for detecting land cover change have been proposed. They include multitemporal classification, image differencing/rationing, vegetation index differencing, principal component analysis and change vector analysis. Various methods for change detection are in detail reviewed by A.Singh (Singh, 1989).

In this study, another approach is described that uses the relative atmospheric correction of multi-temporal satellite images. Relative atmospheric effects between satellite images taken at different times, such as the radiance change arising from the difference in atmospheric conditions and sun angles, can be estimated in a relative way, by taking one image as reference (Caselles, 1989).
First, it is derived from the radiative transfer model that the relation between radiance values of remotely sensed data acquired at two different dates has a linear form. The coeffients of this linear equation only include atmospheric parameters at different times, and are estimated by using radiance values of ground objects which are assumed to have almost constant reflectances with time.The spectral surface reflectance ratio, A(t2)/A(t1), at two different times, t1 and t2, is obtained from count levels of the corresponding pixel in two different images, X(t2) and X(t1), the coefficients of the linear equation and the additive path radiance in the image taken as reference (Kusaka, 1994). The additive path radiance is estimated as the minimum count level at the reference image. Next, the change detection using the surface reflectance ratio at two different times is performed. To do that, the distance d of A(t2)/A(t1) from the value of 1 was introduced. The change detection method in this study depends on the selection of the threshold value of d and therefore the threshold of d was automatically determined by using the 2-dimensional frequency distribution of distance values in two different spectral bands. Finally, the present method was applied to Landsat TM images taken on Oct. 10, 1987 and Nov. 6, 1991. Two images are taken at the same season, and at time intervals of 4 years. This area covers the suburban area near Kanazawa city in Japan. By taking the image of Oct. 1987 as reference, the relative atmospheric correction in the paired images was performed, and the areas of land cover change in the study site were detected by using the relative atmospheric correction images.

2. RELATIVE ATMOSPHERIC CORRECTION

Consider a radiative transfer in a plane-parallel atmosphere bounded by a flat reflecting layer with non-uniform Lambertian reflectance. The upward normal radiance at the top of the atmosphere, L_T, is approximately expressed in a quadratic form with respect to the surface reflectance (Kawata, et al., 1988, Kawata et al., 1990). L_T is given by

$$L_T = (T + SA)A_t + (Q - T)A + (P - S)A^2 + R \qquad (1)$$

where the coefficients P, Q, R, S and T are expressed by the transmission and reflection function in the free atmosphere,

A_t is the surface reflectance of the target object and A the mean background reflectance. As far as the optical thickness of the atmosphere $\tau < 1.0$ and surface reflectance < 0.5, L_T has a linear form with respect to the surface reflectance (Kawata, et al., 1988). Furthermore, it is reasonable to assume A_t=A unless the difference of the reflectance between the target and its surrounding area is enough large to cause the adjacent effects.

Eq.(1) is rewritten as

$$L_T = QA + R \quad (2)$$

If the conversion of the count level of a pixel, X, into the spectral radiance, L_T, is given by $L_T = GX + O$, where G and O are the gain and offset values of the sensor, Eq.(2) is expressed as

$$X = pA + q \quad (3)$$

where p = Q/G and q = (R-O)/G.

Now, let X_1 be the count level of a pixel in the image taken at the time t1and X_2 the count level of the corresponding pixel in the image taken at the time t2. Assuming that the surface reflectance of X_1 is almost the same as that of X_2, the following linear relation is obtained.

$$X_2 = p'X1 + q' \quad (4)$$

where p' = p(t2)/p(t1) and q' = q(t2) - p'q(t1).

The coefficients, p' and q', only include atmospheric parameters and can be estimated if we can identify several objects in two different images that have almost same surface reflectances.

The spectral surface reflectance ratio, A(t2)/A(t1), at two different times, t1 and t2, is therefore expressed as

$$\frac{A(t2)}{A(t1)} = \frac{1}{p'} \frac{X_2 - q' - p'q(t1)}{X_1 - q(t1)} \quad (5)$$

In Eq.(5) unknown factor is only q(t1). As known from Eq.(3), q(t1) is proportional to the additive path radiance and is estimated from the minimum count level X_0 in the image taken as reference. It is found that the relative atmospheric correction between thye images taken at different times is performed by Eq.(5).

2.1 Regression Line

To estimate the coefficients of Eq.(4), we selected the surface objects whose reflectances will be unchangeable with time to determine the regression line by taking the count level of a target in the image on Oct. 10, 1987 as an independent variable. Fig.1 shows Landsat TM images in the study site taken at Nov. 1991. The study site mainly consists of the sea (Sea of Japan; upper-left portion in Fig.1), urban area (central portion), forest (upper-right and lower-right portion) and rice field (lower-left portion). Roads and rivers are also in visible in Fig.1. We chose some pixels corresponding to sea water, urban area, road, railway, residential area from the paired images and computed the mean count levels for the sampled objects in each band. Thus obtained regression line is expressed as

$$X_2 = P'X_1 + Q' \quad (6)$$

where P' and Q' are the estimated values of p' and q', respectively. The estimated values of P' and Q' and the correlation coefficients are shown in Table 1. We can see from Table 1 that the correlation between X_1 and X_2 is very high in every spectral band.

Table 1 Values of Coeffients, P' and Q', of the Regression Line and Correlation Coefficients

TM band	Slope(P')	Intercept (Q')	Correlation
1	0.597	14.0	0.989
2	0.580	5.90	0.983
3	0.676	2.50	0.990
4	0.752	- 0.03	0.996
5	0.739	0.11	0.997
7	0.751	0.15	0.984

2.2 Distribution of Reflectance Ratio

In order to estimate the spectral reflection ratio given by Eq.(5), we carried out the geometrical correction between two Landsat TM images by using ground control points. After that, we computed the value of reflectance ratio in every pixel of paired images by using the values of P' and Q' in Table 1 and minimum count levels in the image of Oct., 1987 taken as reference. Fig.2 shows the frequency distributions of reflectance ratio at bands 2, 3 and 7. As seen from Fig.2, every histogram shows approximately the normal distribution with the mean value near the reflectance ratio 1.

3. CHANGE DETECTION

The spectral reflectance ratio at two diffrent times, t1 and t2, is considered to be unity if the surface reflectance of target objects is unchangeable with time. In other words, the values of the reflectance ratio are different from 1 if the reflectance of ground objects under consideration changes at two different times. To detect ground objects whose surface reflectances have changed, we introduced the distance from the value 1 of A(t2)/A(t1).

In this study we defined the distance D as follows:

$$D = \sum_{i=1}^{6} d_i^2 = \sum_{i=1}^{6} ((r_i - 1) / \sigma_i)^2 \quad (7)$$

where d_i^2 is the distance at band i, r_i = A(t2)/A(t1) at band i and σ_i is the root mean square error of r_i from the value 1 in band i. Fig.3 shows the frequency distribution of D in the study area. The value of D in Fig.3 is multiplied by 10.

The most difficult problem in detecting the area of change by using the distance D is to select the threshold value of D. We devised the following two procedures for selecting the threshold of D: (1) the threshold selection using sample objects that have actually changed at different times and (2) the threshold selection using the 2-dim. frequencies of distance values in two different spectral bands.

3.1 Threshold Selection Using Ground Truth Data

We carried out the ground truth of several regions that actually changed at time intervals of 4 years (1987-1991) and located them in the image under consideration. After that, we determine the threshold of the distance D so that the area of change investigated by the ground truth is successfully detected.

In this study, we selected three different areas of change:

1) newly developed residential area in the mountain,
2) newly constructed factory in the rice field, and
3) newly extended road in the rice field.

And then we computed the mean values of D, D_1, D_2, D_3 for each of three areas, 1), 2) and 3). The threshold value of D, D_t, was determined as $D_t = \text{Min.}\{D_1, D_2, D_3\}\text{-C}$, where C is an arbitrary small value used for detecting the localized pixel area of change in the image. As a result, we found $D_t = 6.9$ (multiplied by 10). Fig.4 is the image showing the area of change. In Fig.4 white regions represent the area of change.

3.2 Change Detection Using 2-Dim. Histograms

In the procedure for detemining the threshold described in the previous section, the ground truth is needed to find some areas that have actually changed. In this section we describe a method for detecting the area of change automatically. This method is based on the idea that some peaks corresponding to the area of change will occur in a 2-dimensional frequency distribution against two distance variables, d_i and d_j ($i \neq j$). For example, consider the land use change of the vegetation field into the residential area. In this case, the change of reflectance ratio in TM bands 1, 2 and 3 will occur in the areas where land use changed, because for their spectral bands the reflectance of the residential area is larger than that of the vegetation. If we construct the frequency distribution against distance values in two of three bands, it will have significant peaks at the large distance value. This is the reason why we use a two dimensional histograms.

We investigated the shape of histograms for all combinations of TM bands (${}_6C_2 = 15$) to detect the area of change. As a result of it, in all the histograms, more than two significant peaks were found in the region where the value of the distance is large. It will be, therefore, possible to extract the area of change from the reflectance ratio image if we can detect the pixels in the image that distribute around the significant peaks in the histogram. However, it is difficult to extract some peaks from the frequency distribution automatically. For simplicity, we divided the two bands distance space into two regions, **Change Area** and **Non-change Area**, as follows:

Change Area is the outside of the ellipse defined as

$$\frac{d_i^2}{a_i^2} + \frac{d_j^2}{b_j^2} = 1 \qquad (8)$$

where a_i and b_j are the values of d_i and d_j corresponding to the valley (minimum between two peaks) that occurs in frequencies on each axis in band i and band j, respectively.

Non-change Area is the inside of the ellipse given by Eq.(8).

In order to examine which combination of TM bands provides better results in detecting the area of change, we extracted the pixels from the paired images that correspond to Change Area in each of all the histigrams and checked whether the areas 1), 2) and 3) used as ground truth data in the previous section 3.1 are successfully detected.

Consequently, we found the following results.

(1) The combinations of d_1d_2, d_2d_3, d_3d_7 provided better results, because the land use in the study site mainly changes from the agricultural field to the residential area and road.

(2) It is difficult to detect the area of change from histograms whose variables are taken as distance values including bands 4 and 5, because most of the study site consists of the vegetation field such as agricultural area and forest, and so it is difficult to find small peaks in the histogram.

(3) In the case that more than two valleys are found in the histogram, we obtain better results if we select the distance value corresponding to the second valley as a_i or b_j in Eq.(8).

Fig.5 shows the frequency distribution in bands 3 and 7 and Fig.6 is the image showing the area of change extracted from the histogram in bands 3 and 7 (White regions represent the areas of change.)

To compare with the results of the section 3.1, we also used the ground truth data,1), 2) and 3), given in the section 3.1. Fig.7 shows the shape of the extracted area of change. As seen from Fig.7, in the extraction of facory in the case 2), the change detection algorithm described in this section is superior to that in the section 3.1 because the shape of the buildings appears clearly. In the case 3), the present algorithm provides better results, as compared to the change detection method described in the previous section because the chain of pixels in the road is more smooth.

4. CONCLUSIONS

A new change detection method using the relative atmospheric correction of multi-temporal Landsat TM images was described. This method is based on the idea that the surface reflectance ratio, A(t2)/A(t1), at two different times, t1 and t2, is obtained from count levels, X(t2) and X(t1), of the corresponding pixel at two different images and the coefficients of the linear equation derived from the relative atmospheric correction. In order to detect the area of change, the distance d of A(t2)/A(t1) from the value of 1 was introduced and the threshold of d was automatically determined by using the 2-dimensional frequency distribution of distance values in different spectral bands. As a result, it was shown that the values of A(t2)/A(t1) are almost normally distributed around the value 1 in every spectral band. It was also found that the areas of land cover

change are successfully detected by using the change detection algorithm described in this study.

References

Caselles, V and M.J. Lopetz Garcia, 1989. An alternative simple approach to estimate atmospheric correction in multitemporal studies, Int. J. Remote Sensing, 10, pp.1127-1134.

Kawata, Y, S. Ueno and T. Kusaka, 1988. Radiometric correction for atmospheric and topographic effects on Landsat MSS images, Int. J. Remote Sensing, 9, pp.729-748.

Kawata, Y, A. Ohtani, T. Kusaka and S. Ueno, 1990. Classification Accuracy for the MOS-1 MESSR data before and after the atmospheric correction, IEEE TGRS, 28, pp.755-760.

Kusaka, T, T. Kakehi, M. Ohtsuka and Y. Kawata, 1994. Land cover change detection using relative atmospheric correction between multitemporal satellite data, In: Proc. of International Symp. on Noise and Clutter Rejection in Radars and Imaging Sensors, Kawasaki, Japan, pp.603-608.

Fig.1 Landsat TM image in the study area taken on Nov. 6, 1991

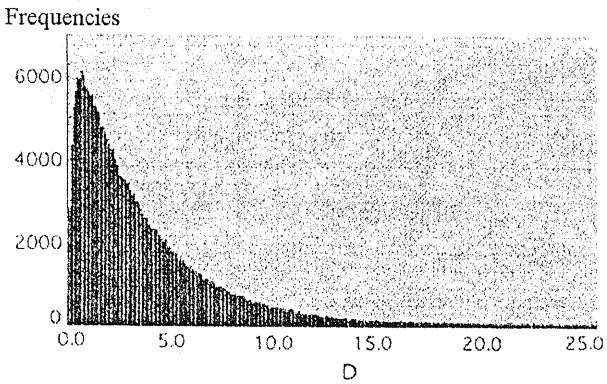

Fig.3 Frequency distribution of the distance D

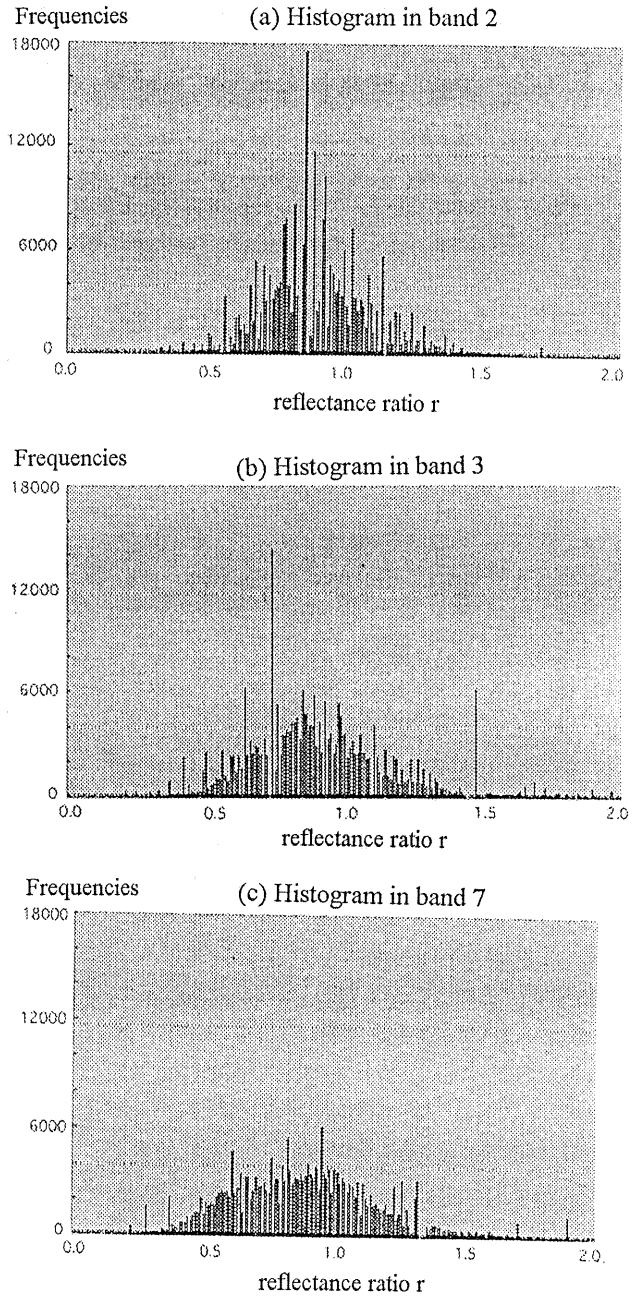

Fig.2 The distribution of the spectral reflectance ratio r=A(1991)/A(1987) (a) Histogram in band 2, (b) Histogram in band 3, (c) Histogram in band 7

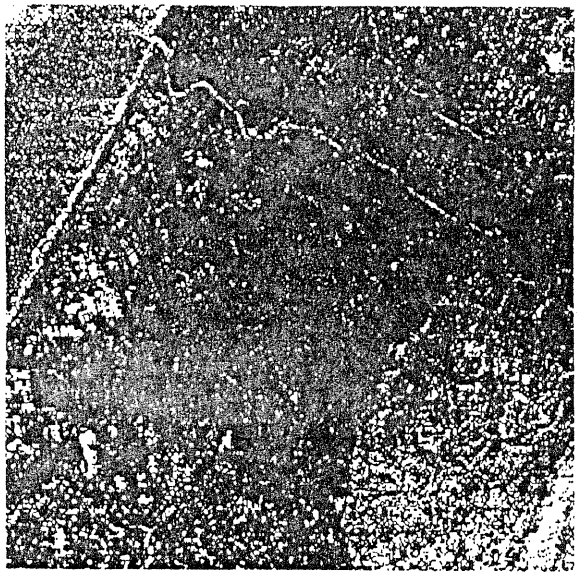

Fig.4 Areas of change (white regions) obtained by the detection algorithm using the threshold value of D

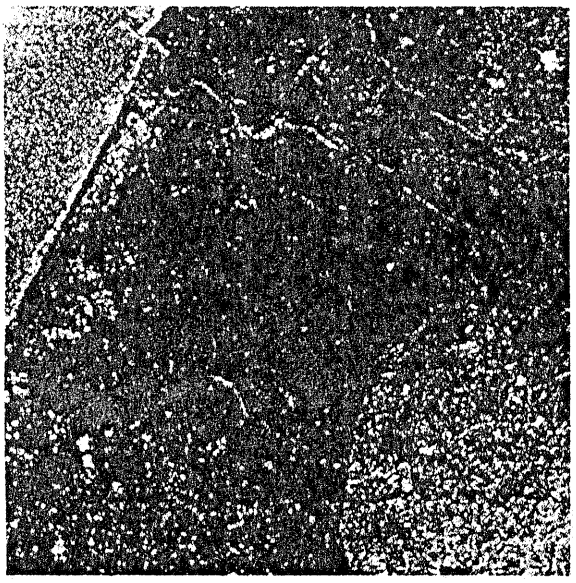

Fig.6. Areas of change (white regions) obtained by the detection algorithm using the 2-dim. histogram

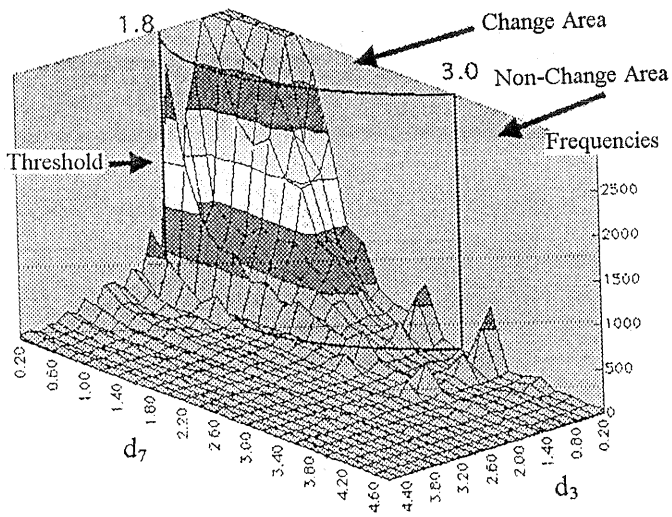

Fig.5 2-dimensional frequency distribution in bands 3 and 7

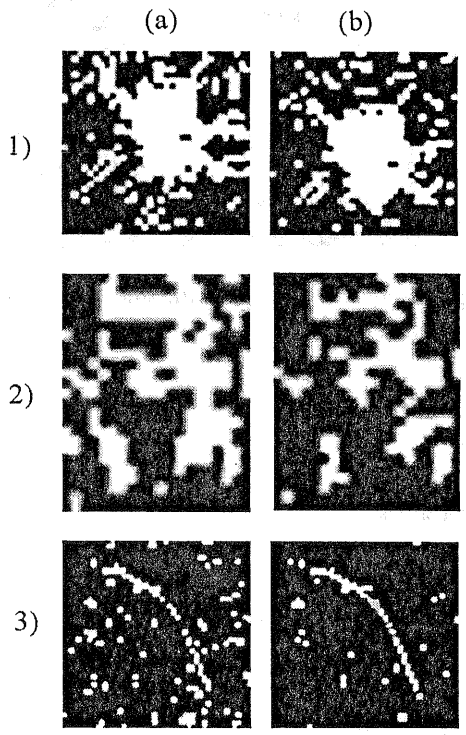

Fig.7 Shape of the pixel areas detected from two methods,
(a) the method using the threshold value of D and
(b) the method using the 2-dim. histogram .
1) newly developed residential area,
2) newly constructed factory, 3) newly extended road